RESEARCH

TNFAIP6 defines the MSC subpopulation with enhanced immune suppression activities

Lingyun Li[1†], Lei Yang[1†], Xian Chen[2†], Xiangjuan Chen[3†], Lianghui Diao[2], Yong Zeng[2] and Jianyong Xu[1,2*]

Abstract

Background: Mesenchymal stromal/stem cells (MSCs) have been intensively investigated in both pre-clinical and clinical studies. However, the therapeutic efficacy varies resulting from the heterogenicity of MSCs. Therefore, purifying the specific MSC subpopulation with specialized function is necessary for their therapeutic applications.

Methods: The large-scale RNA sequencing analysis was performed to identify potential cell markers for the mouse MSCs. Then, the immune suppression activities of the purified MSC subpopulation were assessed in vitro and in vivo.

Results: The TNFAIP6 (tumor necrosis factor alpha-induced protein 6) has been identified as a potential cell marker for mouse MSCs, irrespective of tissue origin and laboratory origin. The TNFAIP6^{+} mouse MSCs showed enhanced immune suppression activities and improved therapeutic effects on the mouse model of acute inflammation, resulting from faster response to immune stimulation.

Conclusions: Therefore, we have demonstrated that the TNFAIP6^{+} MSC subpopulation has enhanced immune suppression capabilities.

Keywords: Mesenchymal stromal/stem cells, MSCs, TNFAIP6, Tumor necrosis factor alpha-induced protein 6, Immune suppression

Introduction

Mesenchymal stromal/stem cells (MSCs) have been intensively investigated in both pre-clinical and clinical studies, because of their multi-potent differentiation and immune modulation capabilities [1–4]. It has been demonstrated that the MSCs or MSC-derived exosomes have therapeutic effects on many diseases [2, 3, 5–7]. Unfortunately, the consistency of their therapeutic efficacy is very low, resulting from the heterogeneity of MSCs [1–3, 8]. Plenty of factors would induce the MSC heterogenicity, such as tissue origin, isolation methods, expansion

medium, and the donor's genetic background, gender, age, and healthy conditions [1, 4, 8–10].

Therefore, delineating the underlying mechanisms and developing novel strategies to target the heterogenicity are necessary to develop MSC-based therapies. Previously, we have developed several strategies to reduce the heterogenicity of MSCs, such as genetic modification [6, 11] and full chemical medium development [5, 12]. On the other hand, purifying specific MSC subpopulations for specific therapeutic purposes is also critical for improving the therapeutic efficacy and consistency, although this is very challenging [1].

Plenty of mouse MSC markers have been demonstrated, including cell surface markers (such as CD105^{+}CD90^{−}, CD90^{+}, CD73^{+}, LepR^{+}, PDGFRα^{+}, PDGFRα^{+}Sca-1^{+}, CD140b/PDGFRβ^{+}, CD51^{+}, Lgr6^{+}, Meflin^{+}, EphA7^{+}, CD49f^{high}, SSEA-4^{+}, p75NTR^{+}, CD44^{+}, CD49e^{+}, CD29^{+}, and Sca-1^{+})[13–33], intracellular markers (such as Gli1, Nestin, Mx1, αSMA, Axin2, Ctsk^{+}Scx^{+}, Hox11, and

†Lingyun Li, Lei Yang, Xian Chen and Xiangjuan Chen have contributed equally to this work and share first authorship

*Correspondence: xujianyong820915@163.com; xujianyong@szu.edu.cn

¹ Department of Immunology, School of Medicine, Health Science Center, Shenzhen University, Nanhai Avenue 3688, Shenzhen 518060, Guangdong, People's Republic of China
Full list of author information is available at the end of the article

Li *et al. Stem Cell Research & Therapy*   (2022) 13:479

Page 2 of 15

Hic1) [34–44], and extracellular/secreted markers (such as Gremlin1, and CXCL12) [45–47]. However, none of these markers are MSC specific. Furthermore, the major therapeutic contributors of the MSC are secreted proteins [2]. Therefore, purifying the specific MSC subpopulation with specialized function is necessary for their therapeutic applications.

In the current study, we performed large-scale RNA sequencing analysis and screened potential cell markers for the mouse MSCs. Our data here demonstrated that TNFAIP6 (tumor necrosis factor alpha-induced protein 6) is a potential cell marker for mouse MSCs, irrespective of tissue origin and laboratory origin. TNFAIP6 is a secreted glycoprotein (around 35kD) with strong immune inhibitory functions and has shown therapeutic effects on immune disorder related diseases, such as acute lung injury, acute pancreatitis, liver injury, colitis, peritonitis, subarachnoid hemorrhage, rheumatoid arthritis, diabetes, and myocardial infarction [48–62]. It is expressed mainly by immune cells and stromal cells, including MSCs, especially when stimulated by pro-inflammatory cytokines, such as TNF-α, IL-1β, IFN-γ, and LPS [57, 63–65]. And the expression level of TNFAIP6 has been developed as a predictor of the therapeutic effects of MSCs in vivo [66]. TNFAIP6 could inhibit neutrophil migration and T helper cell differentiation, promote M2 macrophage polarization and regulatory T cell differentiation, modify ECM, and enhance tight junction [51, 52, 54, 55, 58, 60, 64, 67–69]. And our data here showed that the TNFAIP6$^+$ mouse MSCs have enhanced immune suppression activities and improved therapeutic effects in the mouse model of acute inflammation.

Materials and methods
RNA-seq dataset and analysis
The RNA-seq data used in the current study consist of 185 non-MSC samples from different tissues (Additional file 1: Table S1) and 15 MSC samples (Additional file 2: Table S2). The RNA-seq data were defined as MSC samples when they were described as MSCs in the database and also the corresponding studies (Additional file 2: Table S2), according to the minimal criteria for the MSCs [70]. While the cells were characterized as mature cells, pluripotent cells, or other type of adult stem cells (Additional file 1: Table S1), they were defined as non-MSC samples. The raw RNA-seq data were downloaded from NCBI website (National Center for Biotechnology Information), and analyzed by RSEM (v1.3.3) [71], bowtie 2 (v 2.4.2), and then GC content normalized with EDASeq (v2.28.0) [72], as described previously [12, 73]. The mouse reference genome (version mm39) was used for mapping and RSEM alignment. PCA (principal component analysis) was performed with princomp and ggplot2 packages

in R (v 4.0.0). The RNA-seq data were combined together with Python (v3.8.5150.0), and the tSNE (t-distributed stochastic neighbor embedding) analysis was performed with the Seurat package in R (v 4.0.0). Differential gene expression was conducted with DESeq2 (v 1.34.0) in Bioconductor (v3.14). The GO (Gene Ontology), GO enrichment network, and KEGG (Kyoto Encyclopedia of Genes and Genomes) enrichment were analyzed with the clusterProfiler package (v3.0.4) in R (v 4.0.0).

Mouse experiments
The C57BL/6 J mice (female, 8 weeks old) were purchased from the Guangdong Medical Laboratory Animal Center. The mice were maintained in specific pathogen-free conditions, and this study was approved by the Animal Research Ethics Committee of the School of Medicine, Shenzhen University (A20201241).

Cell isolation from bone marrow, placenta, and fat
Cell isolation was performed as described before with modifications [5, 6, 74]. Briefly, the bone marrow (BM) cells were flushed out of femurs and tibias. Placenta and fat cells were isolated with 4 mg/ml collagenase B and 4 mg/ml dispase (Roche Life Science). Then, the isolated cells were subjected to single-cell RNA sequencing or maintained with DMEM/low glucose (Thermo Fisher Scientific) plus 10% FBS (Thermo Fisher Scientific), 10 ng/ml basic fibroblast growth factor (bFGF, PeproTech), 50 μg/ml ascorbic acid (Selleckchem), and antibiotics (Thermo Fisher Scientific) in cell culture dishes.

Single-cell RNA-seq and analysis
Fresh isolated cells from bone marrow, placenta, and fat were filtered with 40 μm strainer (Corning) and resuspended by 0.04% BSA in HBSS (Thermo Fisher Scientific) at the concentration of 1×10^6 cells/mL. Single-cell GEM (Gel Beads-in-Emulsion) was produced with $10 \times$ Genomics Chromium platform according to the instructions. Finally, the libraries were sequenced with Illumina NovaSeq 6000 System (paired-end mode). Raw data processing, mapping, filtering, and UMI count matrix generation were conducted with 10xGenomics pipeline Cell Ranger (v2.1.0). Then, the gene-cell barcode matrix was further analyzed with Seurat package in R (v 4.0.0).

Flow cytometry
Cell preparation, antibody staining, and flow cytometry were performed as described previously [5, 6]. Briefly, for cell surface protein staining, the freshly isolated cells were incubated with 5% FBS in PBS (Thermo Fisher Scientific) for 30 min, and then, the cells were stained with anti-TNFAIP6 (Cat. No. PA5-75,332, Thermo Fisher

Li *et al. Stem Cell Research & Therapy*   (2022) 13:479

Page 3 of 15

Scientific) for 60 min on ice, followed by 3 times washes, and then FITC-conjugated anti-rabbit IgG secondary (Cat. No. F-2765, Thermo Fisher Scientific) antibody for 30 min. For CD45 staining, the cells were stained with PE-conjugated rat anti-mouse CD45 (Cat. No. 567111, BD Biosciences) or PE Rat IgG2b, κ Isotype Control (Cat. No. 555848, BD Biosciences) for 30 min. For CD44 staining, the cells were stained with FITC-conjugated rat anti-mouse CD44 (Cat. No. 561859, BD Biosciences) or FITC Rat IgG2b, κ Isotype Control (Cat. No. 553988, BD Biosciences) for 30 min. For whole cell protein staining, the cells were fixed with 4% PFA (Paraformaldehyde, Sigma), permeablized with 0.2% Triton-X 100 in PBS with 10% FBS for 30 min, and then subjected to antibody staining. Cells were analyzed with BD AccuriC6 Plus (BD Biosciences), and the data were analyzed with FlowJo software.

TNFAIP6$^+$ cell purification
The freshly isolated BM cells were firstly subjected to CD45$^+$ cell depletion with CD45 MicroBeads (mouse, Miltenyi Biotec) according to the instructions. Then, the CD45$^-$ BM cells were stained the primary antibody to TNFAIP6 (Cat. No. PA5-75,332, Thermo Fisher Scientific). After staining the FITC-conjugated anti-rabbit IgG secondary (Cat. No. F-2765, Thermo Fisher Scientific) antibody for 1 h, the cells were sorted by BD FACSAria SORP cell sorter (BD Biosciences).

Cell proliferation and death analysis
The cell doubling time was assessed as described before [12]. Briefly, the purified TNFAIP6$^+$ or TNFAIP6$^-$ mouse MSCs were plated onto p6 plates at the concentration of 10×10^4 cells per well and expanded with the culture medium [6]. Cells were detached with TrypLE when they reached 80–90% confluence and counted with hemocytometer. The cell death was determined with the Cytotoxicity Detection Kit (Cat. No. 4744934001, Sigma) as described previously [5].

ELISA
The TNFAIP6$^+$ or TNFAIP6$^-$ mouse MSCs were plated onto p12 plates at the concentration of 20×10^4 cells per well. Three days later, the cell culture supernatant was collected and the protein level of TNFAIP6 was measured with mouse TNFAIP6 ELISA kit (Cat. No. CSB-EL023959MO, CUSABIO TECHNOLOGY) according to the instructions.

Peripheral blood was collected from the eyes of the mice, and the serum level of IL-6 (Cat. No. 431304), TNF-α (Cat. No. 430901), IFN-γ (Cat. No. 430801), and IL-1β (Cat. No. 432601) was measured with the ELISA kits (all from BioLegend) according to the instructions.

Splenocytes and MSCs co-culture
The splenocytes were isolated and co-cultured with MSCs as described before with modifications [6]. Briefly, the splenocytes (20×10^4 cells/well) isolated from 8-week-old C57BL/6 J mice were co-cultured with freshly purified TNFAIP6$^+$ or TNFAIP6$^-$ mouse MSCs (5×10^4 cells/well) in 96-well plates with stimulation medium, which contained RPMI1640 plus 10% FBS and $1 \times$ Cell Stimulation Cocktail (all from Thermo Fisher Scientific) for 48 h. Then, the cell proliferation was determined using the Cell Proliferation Kit I (Cat. No.11465007001, Roche), and measured by the automated microplate reader (model 550; Bio-Rad) at 570 nm. The CFSE measurement was performed with CellTrace™ CFSE Cell Proliferation Kit (Thermo Fisher Scientific) according to the instructions.

MSC differentiation
The adipocytes, osteocytes, and chondrocytes differentiation and characterization were performed as previously described [6]. To quantify the adipocyte differentiation efficiency, the Oil Red O was eluted with isopropanol (200μL/well in p12 plate) for 30 min with agitation after lipid droplets staining, and measured by the automated microplate reader (model 550; Bio-Rad) at 490 nm. To quantify the osteocyte differentiation efficiency, the Alizarin Red S was eluted with 10% cetylpyridinium chloride (Sigma, prepared in PBS pH 7.5) at 37 ℃ for 2 h with agitation after calcium staining, and measured by the automated microplate reader (model 550; Bio-Rad) at 405 nm. To quantify the chondrocyte differentiation efficiency, the Alcian Blue was eluted with 6 M guanidine hydrochloride for 3 h with agitation after glycosaminoglycan staining, and measured by the automated microplate reader (model 550; Bio-Rad) at 630 nm.

RNA extraction and qPCR
The RNA extraction, cDNA synthesis, and real-time PCR were performed as previously described [6, 74]. The primer sequences used are shown in Additional file 3: Table S3.

Mouse model of acute inflammation and cell transplantation
The endotoxin-induced acute inflammation mouse model was established as described previously [75]. Briefly, the C57BL/6 J mice (8 weeks old; 20 ± 1 g) were intraperitoneally injected a single dose of 20 mg/kg LPS (Lipopolysaccharides, Cat. No. L5293, Sigma). The TNFAIP6$^+$ or TNFAIP6$^-$ mouse MSCs (1×10^6 cells/mouse) were

Li *et al. Stem Cell Research & Therapy*   (2022) 13:479

Page 4 of 15

transplanted intraperitoneally 30 min before the LPS injection. Each group contained 8 mice.

Lung analysis

Bronchoalveolar lavage (BAL) was performed with cannulating the trachea, washing 3 times with 1 mL PBS containing 0.4 mM EDTA and protease inhibitor mixture (Cat. No. 87786, Thermo Fisher Scientific). After centrifugation at 700 g for 5 min, the supernatant was used for cytokine analysis. The total cell, neutrophil ($CD45^+CD11b^+Ly$-$6G^+Ly$-$6C^{med}$), and $CD45^+$ cells in BAL were measured by flow cytometry. The myeloperoxidase (MPO) activity was quantified with the MPO Activity Assay Kit (Fluorometric, Cat. No. ab111749, Abcam) according to the instructions.

Histological analysis

The lung tissue collection, fixation, tissue processing, embedding, sectioning, and HE (hematoxylin and eosin) staining were performed as described previously [6]. For CD45 staining, the sections were permeablized with 0.2% Triton-X 100 in PBS with 10% FBS for 30 min, followed by rabbit anti-mouse CD45 (Cat. No. ab10558, Abcam) incubation overnight, and detected with the SABC (Rabbit IgG)-POD kit (Cat. No. SA0021, Solarbio).

Statistics

Data were analyzed with SPSS software for Windows (SPSS Inc.) and are shown as mean $\pm$ SEM (standard error of the mean). Two groups comparison was analyzed with Student's *t* test. Multiple groups comparison was analyzed with 1-way ANOVA with normal data distribution, parametric test, and Tukey post hoc tests. $P < 0.05$ was considered statistically significant.

Results

To identify the potential cell marker of the mouse MSCs, which is universal expressed irrespective of tissue origin, development stage, and processing procedures, the total RNA sequencing data were downloaded from NCBI database (https://www.ncbi.nlm.nih.gov/), consisting of different mouse tissues and different types of MSC from different laboratories and tissues (Additional file 1: Table S1 and Additional file 2: Table S2). PCA analysis with R packages showed that most of the MSC samples clustered together (Fig. 1A) and they belonged to the mesoderm lineage (Fig. 1B). However, when comparing the MSCs with fibroblasts, they did not separate into two different populations (Fig. 1C), indicating that they might share some transcriptome similarities or the MSCs were not carefully characterized. Then, the tissue and laboratory origin was labeled (Fig. 1D, E, Additional file 2: Table S2). Although the MSCs from different tissues had

different transcriptome (Fig. 1D), the laboratory origin contributed more to the heterogenicity of MSCs, indicating that the isolation and expansion procedures induced more heterogenicities (Fig. 1E). Then, the RNA sequencing data were integrated together and re-analyzed with another algorithm, tSNE (t-distributed stochastic neighbor embedding). The tSNE analysis showed the similar pattern to the PCA analysis (Fig. 1F–J). To further confirm that the MSC processing procedures induced more heterogenicities than the tissue origin, the primary isolated or in vitro expanded MSCs were labeled. Both PCA and tSNE analysis showed that the in vitro expanded MSCs clustered together much more tightly than the primary isolated MSCs (Fig. 1K, L). Thus, the RNA sequencing data analysis here proposed that the MSC processing procedures might induce more heterogenicities than the tissue origin in the mouse MSCs, indicating that the MSC processing procedures should be standardized in the future. However, the data of the in vitro expanded MSCs were all from the same laboratory (Fig. 1E, K) and contained two different tissue origins (Fig. 1D, K). And this was further confirmed with the tSNE analysis (Fig. 1I, J, L). Therefore, more data and further analysis are needed to confirm this finding.

Then, the differentially expressed genes (DEG) were analyzed. There were totally 812 up-regulated gene and 6821 down-regulated gene in MSCs when comparing with the non-MSCs with the cutoff as log2FC (log2 fold change) > 2 (Additional file 4: Table S4, Additional file 5: Table S5). Among the top 20 highly expressed genes in MSCs, 2 have immune modulation functions (including Mrgprg and Tnfaip6), and 15 are deposited into ECM (extracellular matrix) or secreted (including Has1, Col6a6, Col15a1, Tnfaip6, Fndc1, Clec3b, Dchs2, Sfrp4, Ccl11, Dpt, Col14a1, Abi3bp, Bglap2, Tnn, and C1qtnf2) (Fig. 2A). Among the top 20 down-regulated genes in MSCs, they have quite diverse functions, including AKT pathway regulators (Tcl1b3 and Tcl1), TGF pathway regulator (Foxh1), EGF pathway regulator (Eps8l3), RNA processing (Piwil1), hormone (Sst), cell communication through tight junction (Gjd2), immune regulation (Nlrp14), metabolic regulation (Alppl2 and Spink1), and differentiation regulations (Rfx6 for islet cell differentiation, Cdx1 for enterocyte differentiation, and Tex101 for testis differentiation) (Fig. 2B). Indeed, KEGG and GO enrichment of up-regulated genes in MSCs revealed that these genes enriched in ECM modulation and immune regulation (Fig. 2C–E). Therefore, the MSCs tend to have ECM modulation and immune regulation functions.

Because of the high heterogenicity of MSCs, some potential MSC markers might be neglected by bioinformatic analysis. All these up-regulated genes (Additional file 4: Table S4) in MSCs were plotted by FeaturePlot
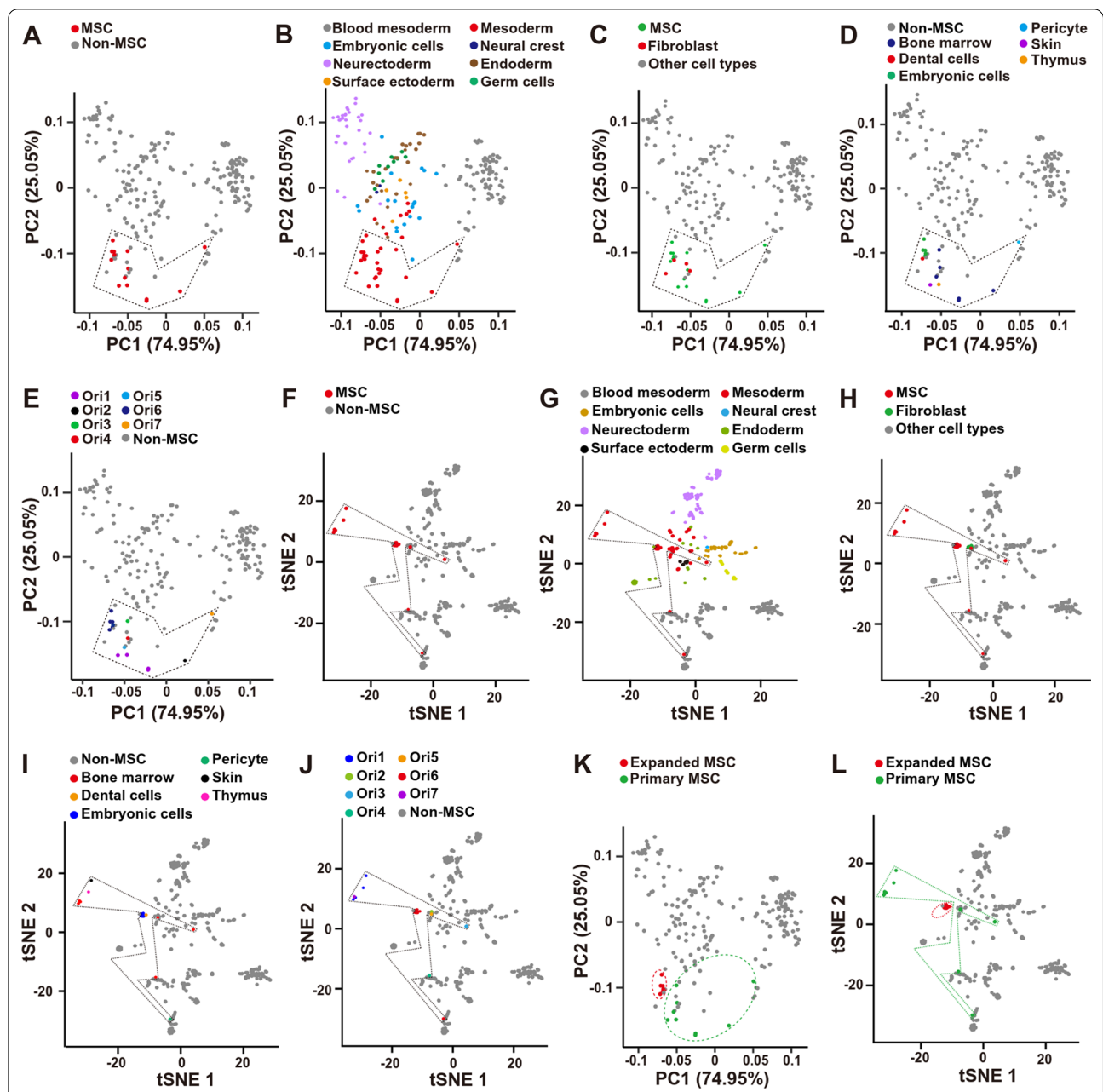
Fig. 1 Bioinformatic analysis of MSCs and non-MSCs RNA-seq data. **A** PCA analysis of MSCs and non-MSCs transcriptome. Red dot indicates MSC samples and they were framed with dash lines. **B** Different germ lineages were labeled in PCA analysis. **C** Fibroblasts (red dot) and MSCs (green dot) were labeled in PCA analysis. **D** MSCs from different tissue origins were labeled in PCA analysis. **E** MSCs from different laboratory origins were labeled in PCA analysis. **F** MSCs and non-MSCs transcriptome was analyzed with tSNE. Red dot indicates MSC samples and they were framed with dash lines. **G** Different germ lineages were labeled in tSNE analysis. **H** Fibroblasts and MSCs were labeled in tSNE analysis. **I** MSCs from different tissue origins were labeled in tSNE analysis. **J** MSCs from different laboratory origins were labeled in tSNE analysis. **K** Expanded and primary MSCs were labeled in PCA analysis. **L** Expanded and primary MSCs were labeled in tSNE analysis. *MSCs* mesenchymal stromal/stem cells; *Ori* laboratory origin

function in R, based on their expression levels. Then, the plotting was manually screened by 3 investigators independently based on the criteria: highly expressed in MSCs and expressed in MSCs from all origins (including different tissues, different laboratories, and fresh isolated or expanded). Finally, 9 potential markers were identified, including Serpinf1, Col1a1, Fkbp10, Rcn3, Col6a2, Gpx8, Mmp2, Ccl2, and Tnfaip6 (Figs. 1F, 3A, Additional

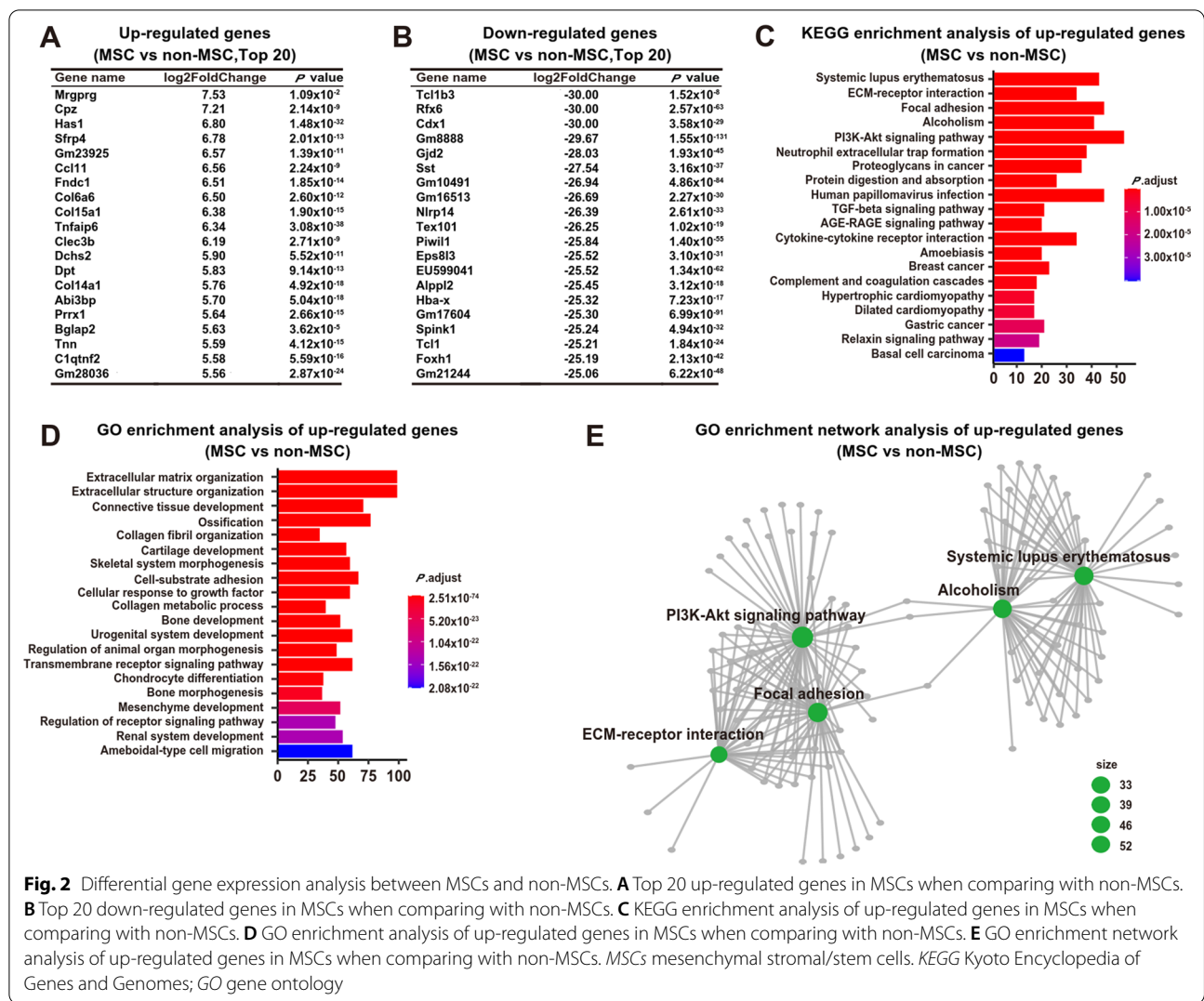Li *et al. Stem Cell Research & Therapy*   (2022) 13:479

Page 6 of 15

Fig. 2 Differential gene expression analysis between MSCs and non-MSCs. **A** Top 20 up-regulated genes in MSCs when comparing with non-MSCs. **B** Top 20 down-regulated genes in MSCs when comparing with non-MSCs. **C** KEGG enrichment analysis of up-regulated genes in MSCs when comparing with non-MSCs. **D** GO enrichment analysis of up-regulated genes in MSCs when comparing with non-MSCs. **E** GO enrichment network analysis of up-regulated genes in MSCs when comparing with non-MSCs. *MSCs* mesenchymal stromal/stem cells. *KEGG* Kyoto Encyclopedia of Genes and Genomes; *GO* gene ontology
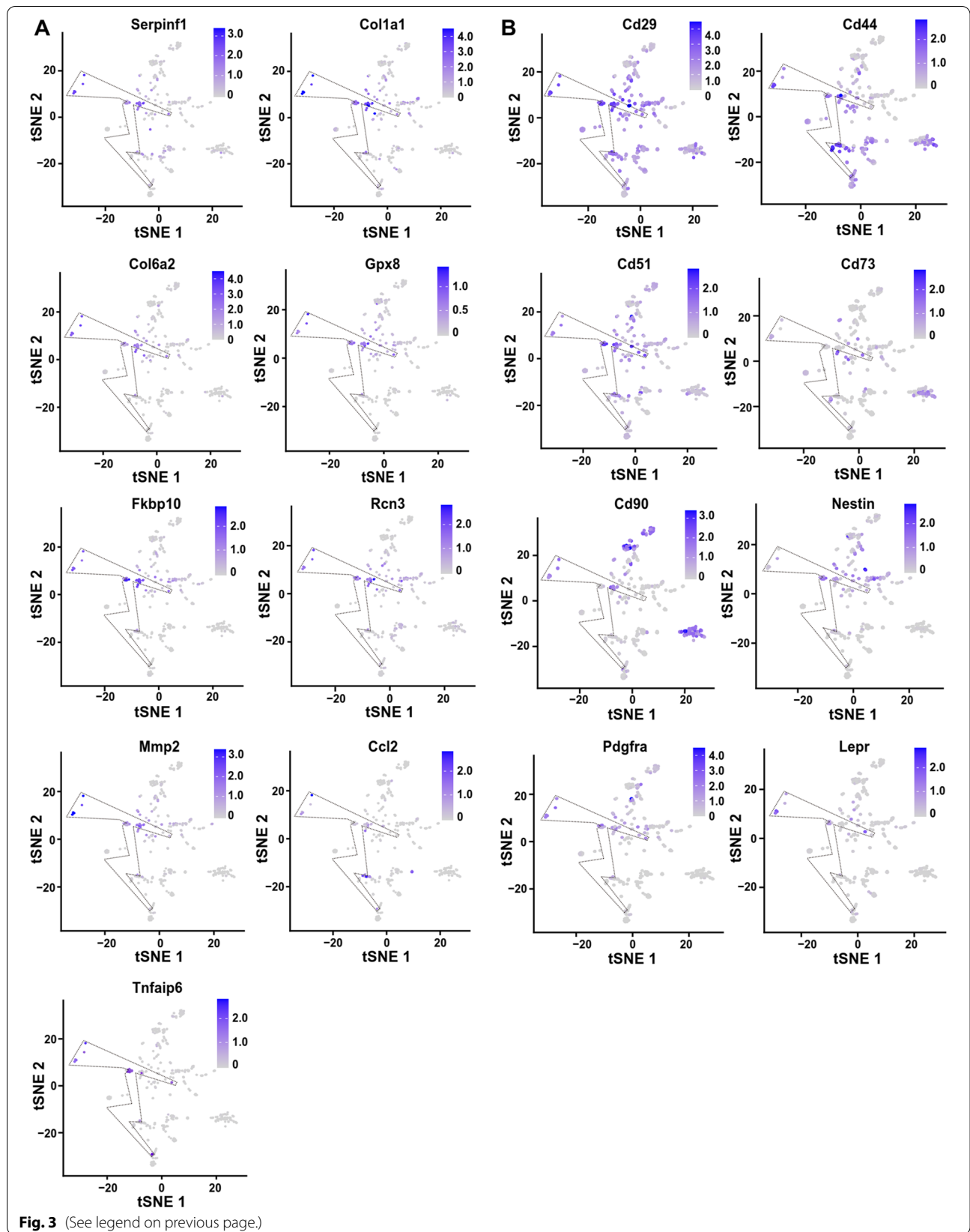
file 6: Table S6). Interestingly, the Tnfaip6 was identified with both bioinformatic analysis (Fig. 2A) and manually screening (Fig. 3A) and exclusively highly expressed in MSCs in the quiescent state (Figs. 1F, 3A). In addition, the known mouse MSC markers were also plotted, including Cd44, Pdgfra, Lepr, Nestin, Cd29, and Cd51 (Fig. 3B). All these known mouse MSC markers were either expressed in non-MSCs, low expressed in MSCs or not expressed in most types of MSCs from all origins (Fig. 3B), indicating that these markers are not MSC specific. Furthermore, the lineage specific genes were not expressed in MSCs, except that the CD34 was expressed in some MSC
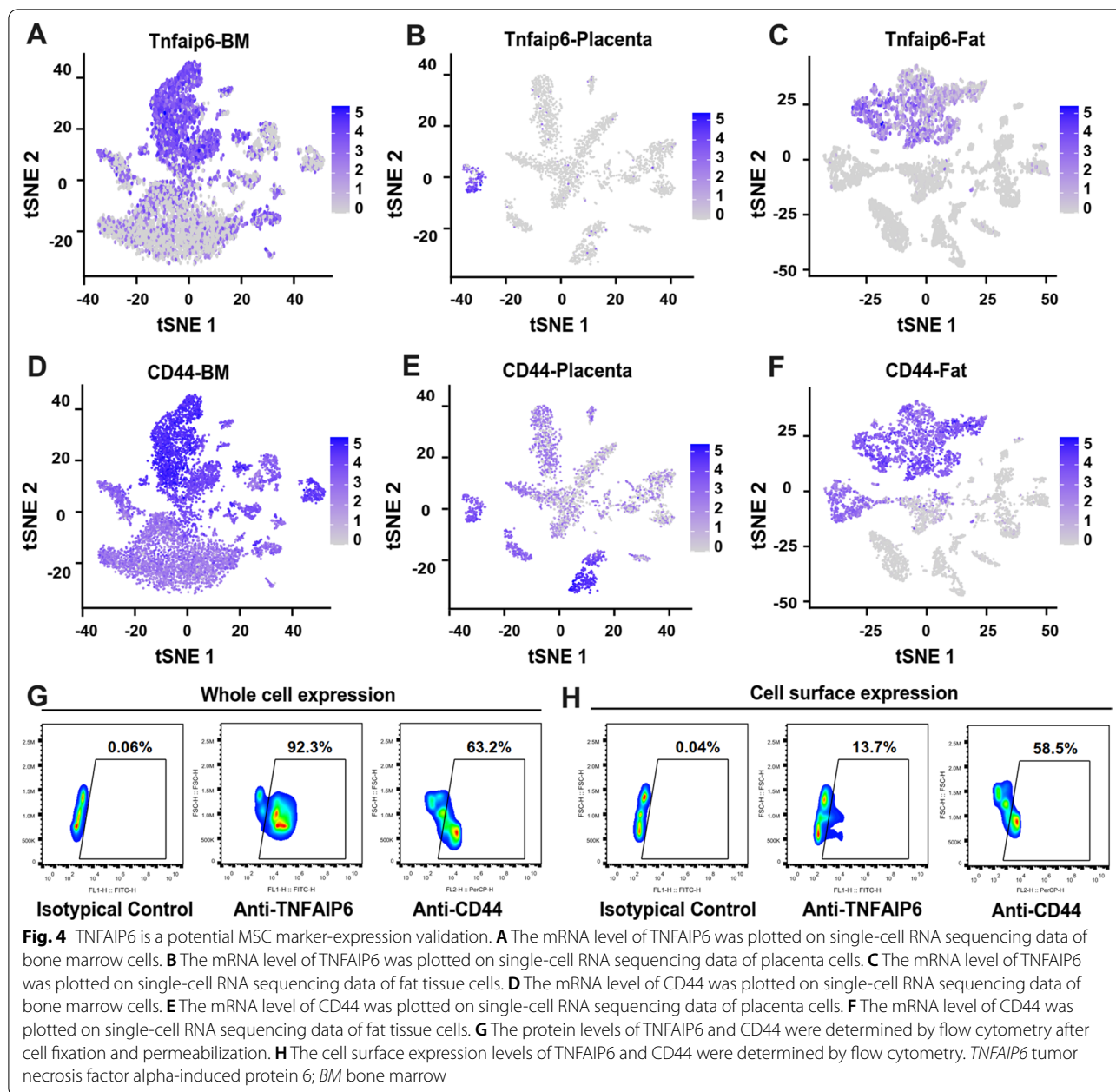
samples with low levels (Additional file 7: Fig. S1). Therefore, the Tnfaip6 is a potential MSC marker.

To further confirm that the Tnfaip6 is a potential MSC marker uncovered by RNA sequencing data analysis, the fresh isolated cells from bone marrow, placenta, and fat tissues were subjected to single-cell RNA sequencing. Data showed that the Tnfaip6 was expressed in all these three types of tissues (Fig. 4A–C). In the meantime, the expression of mouse MSC marker CD44 was also detected (Fig. 4D–F) [6]. Furthermore, the expression of TNFAIP6 and CD44 was also detected at the protein levels by flow cytometry in the bone marrow cells after

(See figure on next page.)

Fig. 3 Tnfaip6 is a potential MSC marker—bioinformatic feature plotting. **A** Plotting of potential MSC marker genes. **B** Plotting of known MSC marker genes. *Serpinf1* serpin family F member 1; *Col1a1* collagen type I alpha 1 chain; *Col6a2* collagen type 6 alpha 2 chain; *Gpx8* glutathione peroxidase 8; *Fkbp10* FK506 binding protein prolyl isomerase 10; *Rcn3* reticulocalbin 3; *Mmp2* matrix metallopeptidase 2; *Ccl2* C–C motif chemokine ligand 2; *Tnfaip6* tumor necrosis factor alpha-induced protein 6; *Pdgfra* platelet-derived growth factor receptor alpha; and *Lepr* leptin receptor

Li *et al. Stem Cell Research & Therapy*   (2022) 13:479

Page 7 of 15

Fig. 3 (See legend on previous page.)

Li *et al. Stem Cell Research & Therapy*   (2022) 13:479

Page 8 of 15

Fig. 4 TNFAIP6 is a potential MSC marker-expression validation. **A** The mRNA level of TNFAIP6 was plotted on single-cell RNA sequencing data of bone marrow cells. **B** The mRNA level of TNFAIP6 was plotted on single-cell RNA sequencing data of placenta cells. **C** The mRNA level of TNFAIP6 was plotted on single-cell RNA sequencing data of fat tissue cells. **D** The mRNA level of CD44 was plotted on single-cell RNA sequencing data of bone marrow cells. **E** The mRNA level of CD44 was plotted on single-cell RNA sequencing data of placenta cells. **F** The mRNA level of CD44 was plotted on single-cell RNA sequencing data of fat tissue cells. **G** The protein levels of TNFAIP6 and CD44 were determined by flow cytometry after cell fixation and permeabilization. **H** The cell surface expression levels of TNFAIP6 and CD44 were determined by flow cytometry. *TNFAIP6* tumor necrosis factor alpha-induced protein 6; *BM* bone marrow

fixation and permeabilization (Fig. 4G). However, the cell surface level of TNFAIP6 was dramatically reduced (Fig. 4H), which is in accordance with previous findings that the TNFAIP6 is a secreted protein [64].

Then, the TNFAIP6$^+$ MSCs were purified with FACS (fluorescence-activated cell sorting) after eliminating the CD45$^+$ lymphocytes with MACS (magnetic-activated cell sorting). The CD45$^-$TNFAIP6$^+$ and CD45$^-$TNFAIP6$^-$ MSCs showed different morphology (Fig. 5A). And the CD45$^-$TNFAIP6$^+$ MSCs expressed higher levels of TNFAIP6 at both mRNA and protein levels (Fig. 5B, C).

They suppressed the lymphocytes proliferation more significantly with dose-dependent effects (Fig. 5D, E). It has been demonstrated that the TNFAIP6 is one of the key factors to maintain the stem cell characteristics of mouse MSCs [76], and thus, we further compared the stem cell characteristics between the CD45$^-$TNFAIP6$^+$ and CD45$^-$TNFAIP6$^-$ MSCs. The data showed that the CD45$^-$TNFAIP6$^+$ MSCs had higher level of CD44 expression (Fig. 5F), proliferation rate (Fig. 5G), and the efficiency of differentiating into adipocytes (Fig. 5H, I), osteocytes (Fig. 5J, K), and chondrocytes (Fig. 5L, M).

Li *et al. Stem Cell Research & Therapy*   (2022) 13:479

Page 9 of 15

Therefore, the TNFAIP6$^+$ MSCs had enhanced immune suppression activities.

To further validate the enhanced immune suppression function of TNFAIP6$^+$ MSCs in vivo, the mouse model of acute inflammation was established via intraperitoneal injection of LPS. Indeed, the TNFAIP6$^+$ MSCs reduced the serum levels of pro-inflammatory cytokines (IL-6, TNF-α, IFN-γ, and IL-1β) (Fig. 6A), total cell number (Fig. 6B), and neutrophil infiltration (Fig. 6C, D) more significantly than the TNFAIP6$^-$ MSCs at 24 h post-LPS stimulation. Furthermore, the TNFAIP6$^+$ MSCs promoted the lung recovery through reducing lymphocytes infiltration (Fig. 6E) and maintaining tissue structure (Fig. 6F) more significantly than the TNFAIP6$^-$ MSCs at day 7 after LPS stimulation. The TNFAIP6 could be induced by pro-inflammatory factors, such as TNF-α, IL-1β, IFN-γ, and LPS [57, 63–65]. Therefore, both TNFAIP6$^+$ and TNFAIP6$^-$ MSCs should express TNFAIP6 in *vivo* after LPS stimulation. To uncover the underlying mechanism that the TNFAIP6$^+$ MSCs had enhanced immune suppression activities, the TNFAIP6$^+$ and TNFAIP6$^-$ MSCs were stimulated with pro-inflammatory cytokines (10 ng/mL TNF-α, 10 ng/mL IL-1β, and 10 ng/mL IFN-γ) to mimic the inflammatory environment. Interestingly, the TNFAIP6$^+$ MSCs responded the stimulation more quickly than the TNFAIP6$^-$ MSCs at both mRNA and protein levels (Fig. 7A, B). Previously, we demonstrated that the anti-inflammatory cytokine IL-37 could improve the therapeutic effects of MSCs through promoting their survival in vivo [5, 6]. Therefore, we hypothesized that the TNFAIP6$^+$ MSCs might also have better survival in vivo through its anti-inflammatory activities. Indeed, co-culture assay showed that the TNFAIP6$^+$ MSCs had higher level of cell survival and lower cell death induced by stimulated splenocytes (Fig. 7C). Then, the TNFAIP6$^+$ or TNFAIP6$^-$ MSCs were mixed with Matrigel and injected intraperitoneally. The data showed that the TNFAIP6$^+$ MSCs recruited less lymphocytes than TNFAIP6$^-$ MSCs (Fig. 7D). Therefore,

the TNFAIP6$^+$ MSCs might respond to the inflammatory environment and secrete the anti-inflammatory cytokine TNFAIP6 more quickly, resulting in immediately immune suppression and less MSC death induced by activated immune cells. The survived MSCs express more anti-inflammatory cytokines and further enhance the immune suppression function (Fig. 7E). In summary, we demonstrated that the TNFAIP6$^+$ MSCs had enhanced immune suppression capabilities (Fig. 7F).

Discussion

The therapeutic inconsistency of MSCs significantly hampers their large-scale clinical applications [1–3, 8]. Therefore, reducing the MSC heterogenicity and improving their therapeutic consistency are critical and urgently needed [1, 4, 8]. Among different strategies, identifying and purifying specific MSC subpopulation with specific functions is a promising strategy to reduce the MSC heterogenicity and improve their therapeutic consistency [1]. Through lineage tracing and function validation, many different makers were identified for the mouse MSCs [13–47]. However, these markers are not MSC specific. And most of them are also not related to their functions and therapeutic efficacy, or the underlying mechanism linking the MSC marker to the function is missing. Therefore, identifying and purifying specific MSC subpopulation with specific function is necessary for their therapeutic applications.

In the current study, the purified CD45$^-$TNFAIP6$^+$ mouse MSCs showed enhanced immune suppression activities and improved therapeutic effects in the mouse model of acute inflammation. Although direct application of recombinant TNFAIP6 protein also has significant therapeutic effects in several mouse models [75, 77–80], similar to our previous investigations on the therapeutic effects of IL-37[6], the TNFAIP6 protein also has a very short half-life in vivo (around 0.2 h) [77]. The TNFAIP6$^+$ MSCs respond to the inflammatory environment and secrete the anti-inflammatory cytokine TNFAIP6 more

(See figure on next page.)

Fig. 5 TNFAIP6 defines a subpopulation of mouse MSCs with enhanced immune suppression activities. **A** Cell morphology of CD45$^-$TNFAIP6$^-$ and CD45$^-$TNFAIP6$^+$ MSCs. **B** Left panel: mRNA level of TNFAIP6 was assessed by qPCR (n = 3); Right panel: protein level of TNFAIP6 was assessed by western blot. **C** Protein level of TNFAIP6 secreted from the CD45$^-$TNFAIP6$^-$ or CD45$^-$TNFAIP6$^+$ MSCs (n = 3). **D** Splenocytes proliferation assay after co-culture with CD45$^-$TNFAIP6$^-$ or CD45$^-$TNFAIP6$^+$ MSCs (n = 3). Both high cell number (5×10^4) and low cell number (2×10^4) were assessed. **E** Splenocytes proliferation assay after co-culture with CD45$^-$TNFAIP6$^-$ or CD45$^-$TNFAIP6$^+$ MSCs was assessed with CFSE approach. High cell number (5×10^4) was used. **F** CD44 expression of CD45$^-$TNFAIP6$^-$ or CD45$^-$TNFAIP6$^+$ MSCs, determined by flow cytometry. **G** Cell proliferation of CD45$^-$TNFAIP6$^-$ or CD45$^-$TNFAIP6$^+$ MSCs was determined by doubling time (n = 3). **H** The adipocytes differentiation efficiency was assessed by Oil Red O staining. **I** The adipocytes differentiation efficiency was quantified by Oil Red O staining and qPCR analysis of gene Lpl and Ppar γ (n = 3). **J** The osteocytes differentiation efficiency was assessed by Alizarin Red staining. **K** The osteocytes differentiation efficiency was quantified by Alizarin Red staining and qPCR analysis of gene Osterix and Runx2 (n = 3). **L** The chondrocytes differentiation efficiency was assessed by Alcian Blue staining. **M** The chondrocytes differentiation efficiency was quantified by Alcian Blue staining and qPCR analysis of gene Sox9 and Bmp2 (n = 3). * indicates *P* < 0.05. *TNFAIP6* tumor necrosis factor alpha-induced protein 6; *MSCs* mesenchymal stromal/stem cells; *Lpl* lipoprotein lipase; *Ppar*γ peroxisome proliferator-activated receptor gamma; *Osterix* Sp7 transcription factor; *Runx2* RUNX family transcription factor 2; *Sox9* SRY-box transcription factor 9; and *Bmp2* bone morphogenetic protein 2
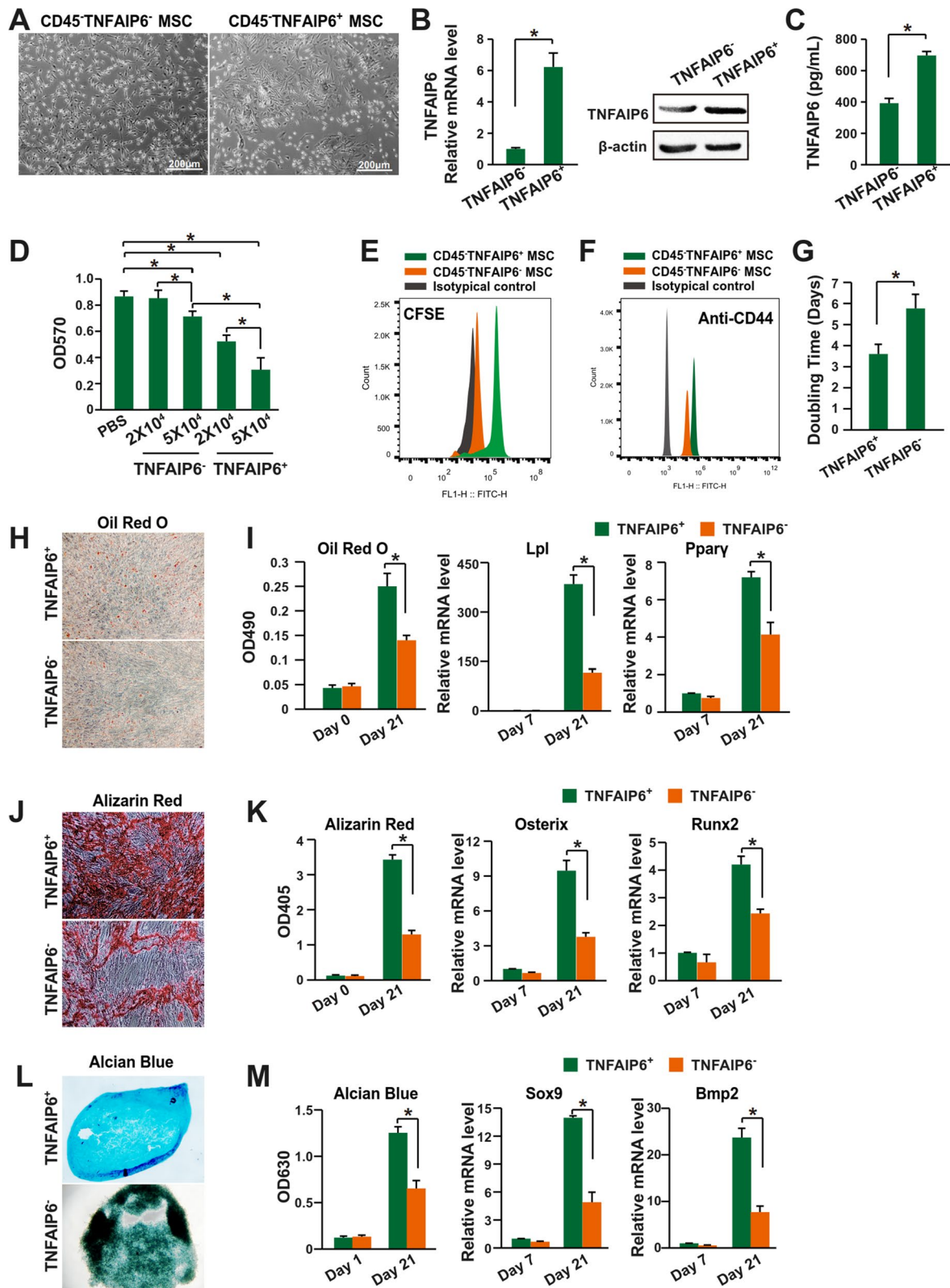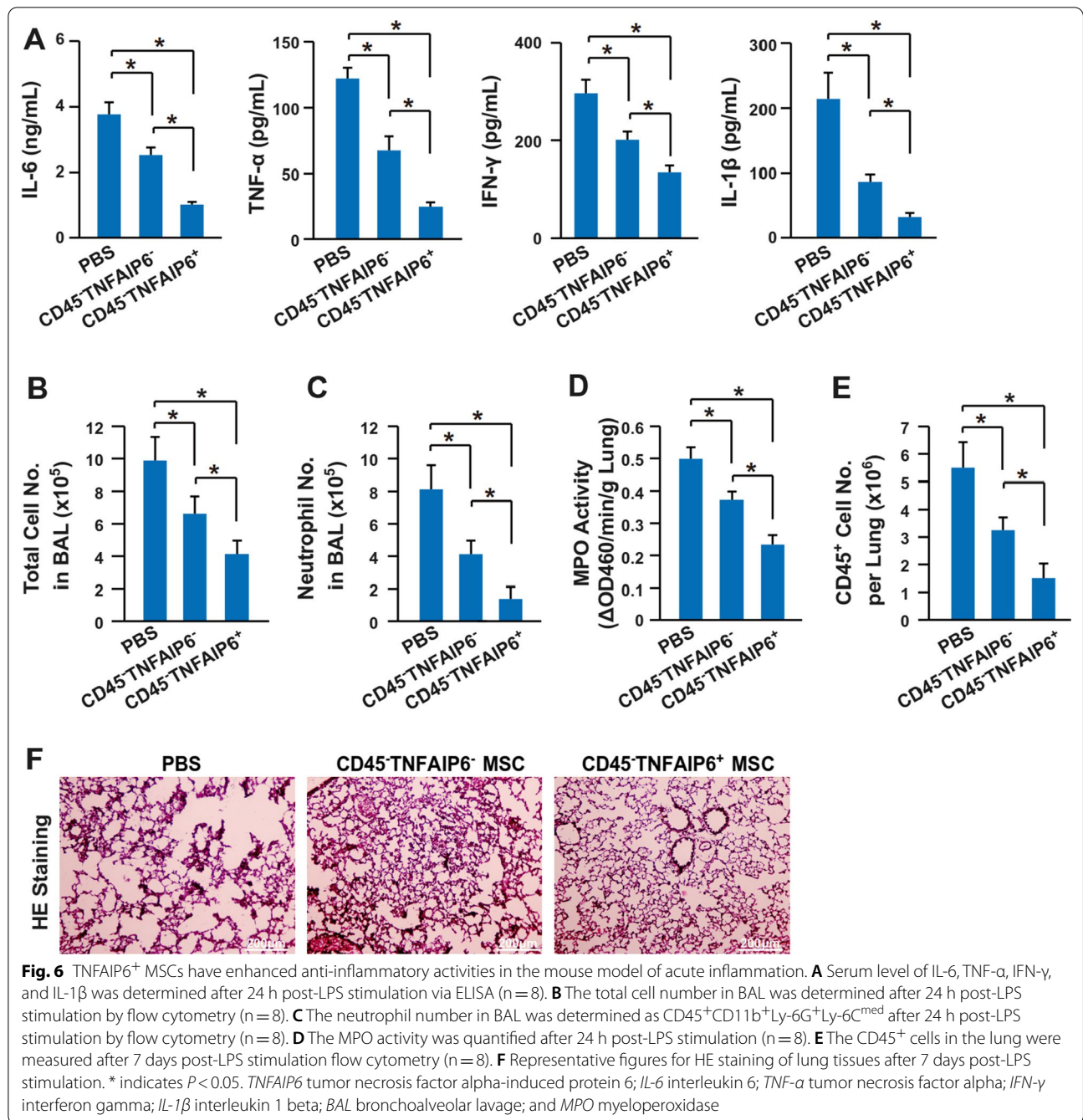
Li *et al. Stem Cell Research & Therapy*   (2022) 13:479

Page 10 of 15

Fig. 5 (See legend on previous page.)

Fig. 6 TNFAIP6$^+$ MSCs have enhanced anti-inflammatory activities in the mouse model of acute inflammation. **A** Serum level of IL-6, TNF-α, IFN-γ, and IL-1β was determined after 24 h post-LPS stimulation via ELISA (n = 8). **B** The total cell number in BAL was determined after 24 h post-LPS stimulation by flow cytometry (n = 8). **C** The neutrophil number in BAL was determined as CD45$^+$CD11b$^+$Ly-6G$^+$Ly-6C^{med} after 24 h post-LPS stimulation by flow cytometry (n = 8). **D** The MPO activity was quantified after 24 h post-LPS stimulation (n = 8). **E** The CD45$^+$ cells in the lung were measured after 7 days post-LPS stimulation flow cytometry (n = 8). **F** Representative figures for HE staining of lung tissues after 7 days post-LPS stimulation. * indicates *P* < 0.05. *TNFAIP6* tumor necrosis factor alpha-induced protein 6; *IL-6* interleukin 6; *TNF-α* tumor necrosis factor alpha; *IFN-γ* interferon gamma; *IL-1β* interleukin 1 beta; *BAL* bronchoalveolar lavage; and *MPO* myeloperoxidase

quickly, resulting in immediately immune suppression and less MSC death induced by activated immune cells. And the survived MSCs express high level of anti-inflammatory cytokines, which further enhances the immune suppression function as positive feedback.

Conclusions

In conclusion, we have identified TNFAIP6 as a new MSC marker and the TNFAIP6$^+$ MSC subpopulation has enhanced immune suppression capabilities.
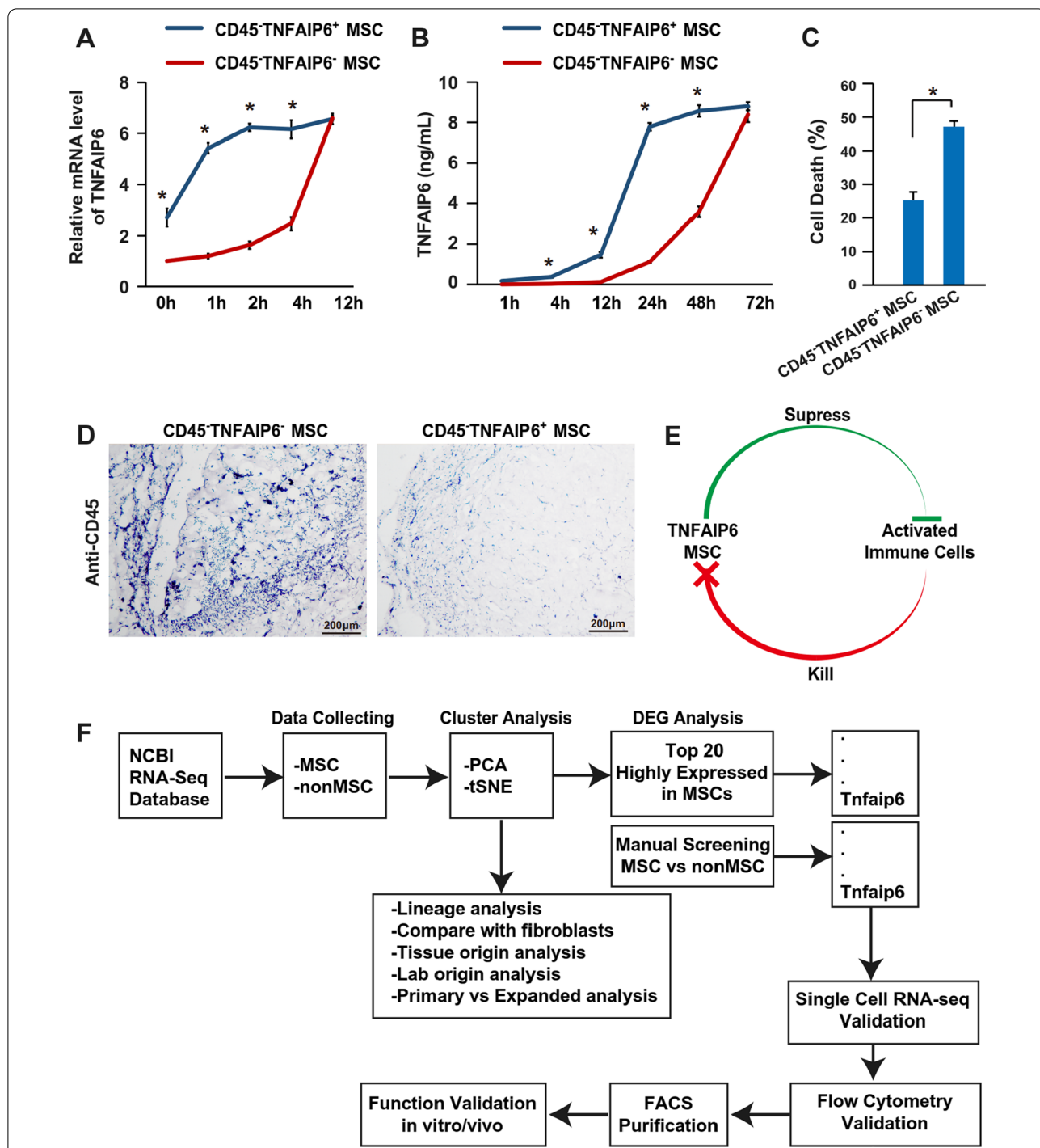
Fig. 7 TNFAIP6^{+} MSCs are resistant to immunologic cytotoxicity through faster response to immune stimulation. **A** The mRNA level of TNFAIP6 was determined via qPCR after stimulated with 10 ng/mL TNF-α, 10 ng/mL IL-1β, and 10 ng/mL IFN-γ for 48 h (n = 3). **B** The protein level of TNFAIP6 was determined via ELISA after stimulated with 10 ng/mL TNF-α, 10 ng/mL IL-1β, and 10 ng/mL IFN-γ for 48 h (n = 3). **C** Cytotoxicity was detected by measuring LDH secretion after co-culture with stimulated splenocytes (n = 3). **D** Representative lymphocytes infiltration within in the Matrigel plug containing TNFAIP6⁻ or TNFAIP6⁺ MSCs at day 3 post-cell transplantation. **E** Proposed potential mechanism of enhanced immune suppression activities of TNFAIP6⁺ MSCs. **F** Representation of the process to identify the TNAFAIP6 as a MSC marker. * indicates *P < 0.05*. *TNFAIP6* tumor necrosis factor alpha-induced protein 6; *MSCs* mesenchymal stromal/stem cells; and *LDH* lactate dehydrogenase

Li *et al. Stem Cell Research & Therapy*   (2022) 13:479

Page 13 of 15

Abbreviations

MSCs: Mesenchymal stromal/stem cells; TNFAIP6: Tumor necrosis factor alpha-induced protein 6; PCA: Principal component analysis; tSNE: t-distributed stochastic neighbor embedding; GO: Gene ontology; KEGG: Kyoto Encyclopedia of Genes and Genomes; BM: Bone marrow; FBS: Fetal bovine serum; bFGF: Basic fibroblast growth factor; PFA: Paraformaldehyde; BAL: Bronchoalveolar lavage; MPO: Myeloperoxidase; HE: Hematoxylin and eosin; DEG: Differentially expressed genes; Log2FC: Log2 fold change; ECM: Extracellular matrix.

Supplementary Information

The online version contains supplementary material available at https://doi.org/10.1186/s13287-022-03176-5.

Additional file 1: Basic information of non-MSC samples.

Additional file 2: Basic information of MSC samples.

Additional file 3: qPCR primer sequences.

Additional file 4: Up-regulated genes in MSC vs non-MSC (FC > 2).

Additional file 5: Down-regulated genes in MSC vs non-MSC (FC > -2).

Additional file 6: Manual screening daa.

Additional file 7: Figure 1. Plotting of MSC negative marker genes.

Data availability
The datasets for this study are available on request from the corresponding author.

Declarations

Ethics approval and consent to participate
The mouse study was approved by the Animal Research Ethics Committee of the School of Medicine, Shenzhen University.

Consent for publication
Not applicable.

Competing interests
The authors declare that the research was conducted in the absence of any commercial or financial relationships that could be construed as a potential conflict of interest.

Author details
[1]Department of Immunology, School of Medicine, Health Science Center, Shenzhen University, Nanhai Avenue 3688, Shenzhen 518060, Guangdong, People's Republic of China. [2]Shenzhen Key Laboratory for Reproductive Immunology of Peri-Implantation, Shenzhen Zhongshan Institute for Reproduction and Genetics, Fertility Center, Shenzhen Zhongshan Urology Hospital, Shenzhen 518060, Guangdong, People's Republic of China. [3]Department of Obstetrics, Shenzhen University General Hospital, Shenzhen University, Shenzhen, People's Republic of China.

References

1. Levy O, Kuai R, Siren EMJ, Bhere D, Milton Y, Nissar N, et al. Shattering barriers toward clinically meaningful MSC therapies. Sci Adv. 2020;6(30):eaba6884.
2. Jiang W, Xu J. Immune modulation by mesenchymal stem cells. Cell Prolif. 2020;53(1): e12712.
3. Xu J. Therapeutic applications of mesenchymal stem cells for systemic lupus erythematosus. Adv Exp Med Biol. 2018;1089:73–85.
4. Wang Y, Chen X, Cao W, Shi Y. Plasticity of mesenchymal stem cells in immunomodulation: pathological and therapeutic implications. Nat Immunol. 2014;15(11):1009–16.
5. Xu J, Lian W, Wu H, Wang X, Chen J, Yang L, et al. Improved therapeutic consistency and efficacy of mesenchymal stem cells expanded with chemically defined medium for systemic lupus erythematosus. Cell Mol Immunol. 2020;17(10):1104–6.
6. Xu J, Chen J, Li W, Lian W, Huang J, Lai B, et al. Additive therapeutic effects of mesenchymal stem cells and IL-37 for systemic Lupus Erythematosus. J Am Soc Nephrol. 2020;31(1):54–65.
7. Galipeau J, Sensebe L. Mesenchymal stromal cells: clinical challenges and therapeutic opportunities. Cell Stem Cell. 2018;22(6):824–33.
8. Costa LA, Eiro N, Fraile M, Gonzalez LO, Saa J, Garcia-Portabella P, et al. Functional heterogeneity of mesenchymal stem cells from natural niches to culture conditions: implications for further clinical uses. Cell Mol Life Sci. 2021;78(2):447–67.
9. Moll G, Ankrum JA, Kamhieh-Milz J, Bieback K, Ringden O, Volk HD, et al. Intravascular mesenchymal stromal/stem cell therapy product diversification: time for new clinical guidelines. Trends Mol Med. 2019;25(2):149–63.
10. Moll G, Ankrum JA, Olson SD, Nolta JA. Improved MSC minimal criteria to maximize patient safety: a call to embrace tissue factor and hemocompatibility assessment of MSC products. Stem Cells Transl Med. 2022;11(1):2–13.
11. Jiang W, Lian W, Chen J, Li W, Huang J, Lai B, et al. Rapid identification of genome-edited mesenchymal stem cell colonies via Cas9. Biotechniques. 2019;66(5):231–4.
12. Xu J, Lian W, Chen J, Li W, Li L, Huang Z. Chemical-defined medium supporting the expansion of human mesenchymal stem cells. Stem Cell Res Ther. 2020;11(1):125.
13. Chan CK, Chen CC, Luppen CA, Kim JB, DeBoer AT, Wei K, et al. Endochondral ossification is required for haematopoietic stem-cell niche formation. Nature. 2009;457(7228):490–4.
14. Li Q, Hou H, Li M, Yu X, Zuo H, Gao J, et al. CD73(+) mesenchymal stem cells ameliorate myocardial infarction by promoting angiogenesis. Front Cell Dev Biol. 2021;9: 637239.
15. Suto EG, Mabuchi Y, Toyota S, Taguchi M, Naraoka Y, Itakura N, et al. Advantage of fat-derived CD73 positive cells from multiple human tissues, prospective isolated mesenchymal stromal cells. Sci Rep. 2020;10(1):15073.
16. An Z, Sabalic M, Bloomquist RF, Fowler TE, Streelman T, Sharpe PT. A quiescent cell population replenishes mesenchymal stem cells to drive accelerated growth in mouse incisors. Nat Commun. 2018;9(1):378.
17. Zhou BO, Yue R, Murphy MM, Peyer JG, Morrison SJ. Leptin-receptor-expressing mesenchymal stromal cells represent the main source of bone formed by adult bone marrow. Cell Stem Cell. 2014;15(2):154–68.
18. Yue R, Zhou BO, Shimada IS, Zhao Z, Morrison SJ. Leptin receptor promotes adipogenesis and reduces osteogenesis by regulating mesenchymal stromal cells in adult bone marrow. Cell Stem Cell. 2016;18(6):782–96.
19. Miwa H, Era T. Tracing the destiny of mesenchymal stem cells from embryo to adult bone marrow and white adipose tissue via Pdgfralpha expression. Development. 2018;145(2).
20. Koide Y, Morikawa S, Mabuchi Y, Muguruma Y, Hiratsu E, Hasegawa K, et al. Two distinct stem cell lineages in murine bone marrow. Stem Cells. 2007;25(5):1213–21.
21. Xie DM, Chen Y, Liao Y, Lin W, Dai G, Lu DH, et al. Cardiac derived CD51-positive mesenchymal stem cells enhance the cardiac repair through SCF-mediated angiogenesis in mice with myocardial infarction. Front Cell Dev Biol. 2021;9: 642533.
22. Xie DM, Li YL, Li J, Li Q, Lu G, Zhai Y, et al. CD51 distinguishes a subpopulation of bone marrow mesenchymal stem cells with distinct migratory potential: a novel cell-based strategy to treat acute myocardial infarction in mice. Stem Cell Res Ther. 2019;10(1):331.

23. Zang ZJ, Wang J, Chen Z, Zhang Y, Gao Y, Su Z, et al. Transplantation of CD51(+) stem leydig cells: a new strategy for the treatment of testosterone deficiency. Stem Cells. 2017;35(5):1222–32.

24. Jiang MH, Cai B, Tuo Y, Wang J, Zang ZJ, Tu X, et al. Characterization of Nestin-positive stem Leydig cells as a potential source for the treatment of testicular Leydig cell dysfunction. Cell Res. 2014;24(12):1466–85.

25. Lehoczky JA, Tabin CJ. Lgr6 marks nail stem cells and is required for digit tip regeneration. Proc Natl Acad Sci USA. 2015;112(43):13249–54.

26. Morikawa S, Mabuchi Y, Kubota Y, Nagai Y, Niibe K, Hiratsu E, et al. Prospective identification, isolation, and systemic transplantation of multipotent mesenchymal stem cells in murine bone marrow. J Exp Med. 2009;206(11):2483–96.

27. Maeda K, Enomoto A, Hara A, Asai N, Kobayashi T, Horinouchi A, et al. Identification of meflin as a potential marker for mesenchymal stromal cells. Sci Rep. 2016;6:22288.

28. Hara A, Kobayashi H, Asai N, Saito S, Higuchi T, Kato K, et al. Roles of the mesenchymal stromal/stem cell marker meflin in cardiac tissue repair and the development of diastolic dysfunction. Circ Res. 2019;125(4):414–30.

29. Yoshida Y, Kabara M, Kano K, Horiuchi K, Hayasaka T, Tomita Y, et al. Capillary-resident EphA7(+) pericytes are multipotent cells with anti-ischemic effects through capillary formation. Stem Cells Transl Med. 2020;9(1):120–30.

30. Yang Z, Ma S, Cao R, Liu L, Cao C, Shen Z, et al. CD49f(high) defines a distinct skin mesenchymal stem cell population capable of hair follicle epithelial cell maintenance. J Investig Dermatol. 2020;140(3):544–55 e9.

31. Gang EJ, Bosnakovski D, Figueiredo CA, Visser JW, Perlingeiro RC. SSEA-4 identifies mesenchymal stem cells from bone marrow. Blood. 2007;109(4):1743–51.

32. Suzuki K, Tanaka M, Watanabe N, Saito S, Nonaka H, Miyajima A. p75 Neurotrophin receptor is a marker for precursors of stellate cells and portal fibroblasts in mouse fetal liver. Gastroenterology. 2008;135(1):270–81 e3.

33. Meirelles Lda S, Nardi NB. Murine marrow-derived mesenchymal stem cell: isolation, in vitro expansion, and characterization. Br J Haematol. 2003;123(4):702–11.

34. Zhao H, Feng J, Ho TV, Grimes W, Urata M, Chai Y. The suture provides a niche for mesenchymal stem cells of craniofacial bones. Nat Cell Biol. 2015;17(4):386–96.

35. Shi Y, He G, Lee WC, McKenzie JA, Silva MJ, Long F. Gli1 identifies osteogenic progenitors for bone formation and fracture repair. Nat Commun. 2017;8(1):2043.

36. Mendez-Ferrer S, Michurina TV, Ferraro F, Mazloom AR, Macarthur BD, Lira SA, et al. Mesenchymal and haematopoietic stem cells form a unique bone marrow niche. Nature. 2010;466(7308):829–34.

37. Liao Y, Li G, Zhang X, Huang W, Xie D, Dai G, et al. Cardiac Nestin(+) mesenchymal stromal cells enhance healing of ischemic heart through periostin-mediated M2 macrophage polarization. Mol Ther. 2020;28(3):855–73.

38. Jiang MH, Li G, Liu J, Liu L, Wu B, Huang W, et al. Nestin(+) kidney resident mesenchymal stem cells for the treatment of acute kidney ischemia injury. Biomaterials. 2015;50:56–66.

39. Park D, Spencer JA, Koh BI, Kobayashi T, Fujisaki J, Clemens TL, et al. Endogenous bone marrow MSCs are dynamic, fate-restricted participants in bone maintenance and regeneration. Cell Stem Cell. 2012;10(3):259–72.

40. Roguljic H, Matthews BG, Yang W, Cvija H, Mina M, Kalajzic I. In vivo identification of periodontal progenitor cells. J Dent Res. 2013;92(8):709–15.

41. Maruyama T, Jeong J, Sheu TJ, Hsu W. Stem cells of the suture mesenchyme in craniofacial bone development, repair and regeneration. Nat Commun. 2016;7:10526.

42. Pineault KM, Song JY, Kozloff KM, Lucas D, Wellik DM. Hox11 expressing regional skeletal stem cells are progenitors for osteoblasts, chondrocytes and adipocytes throughout life. Nat Commun. 2019;10(1):3168.

43. Feng H, Xing W, Han Y, Sun J, Kong M, Gao B, et al. Tendon-derived cathepsin K-expressing progenitor cells activate Hedgehog signaling to drive heterotopic ossification. J Clin Investig. 2020;130(12):6354–65.

44. Scott RW, Arostegui M, Schweitzer R, Rossi FMV, Underhill TM. Hic1 defines quiescent mesenchymal progenitor subpopulations with distinct functions and fates in skeletal muscle regeneration. Cell Stem Cell. 2019;25(6):797–813 e9.

45. Worthley DL, Churchill M, Compton JT, Tailor Y, Rao M, Si Y, et al. Gremlin 1 identifies a skeletal stem cell with bone, cartilage, and reticular stromal potential. Cell. 2015;160(1–2):269–84.

46. Greenbaum A, Hsu YM, Day RB, Schuettpelz LG, Christopher MJ, Borgerding JN, et al. CXCL12 in early mesenchymal progenitors is required for haematopoietic stem-cell maintenance. Nature. 2013;495(7440):227–30.

47. Omatsu Y, Sugiyama T, Kohara H, Kondoh G, Fujii N, Kohno K, et al. The essential functions of adipo-osteogenic progenitors as the hematopoietic stem and progenitor cell niche. Immunity. 2010;33(3):387–99.

48. Abraham C, Cho JH. Inflammatory bowel disease. N Engl J Med. 2009;361(21):2066–78.

49. Sala E, Genua M, Petti L, Anselmo A, Arena V, Cibella J, et al. Mesenchymal stem cells reduce colitis in mice via release of TSG6, independently of their localization to the intestine. Gastroenterology. 2015;149(1):163–76 e20.

50. Zhang S, Fang J, Liu Z, Hou P, Cao L, Zhang Y, et al. Inflammatory cytokines-stimulated human muscle stem cells ameliorate ulcerative colitis via the IDO-TSG6 axis. Stem Cell Res Ther. 2021;12(1):50.

51. Wan Y, Song M, Xie X, Chen Z, Gao Z, Wu X, et al. BMSCs Regulate astrocytes through TSG-6 to protect the blood-brain barrier after subarachnoid hemorrhage. Mediators Inflamm. 2021;2021:5522291.

52. Yang S, Liang X, Song J, Li C, Liu A, Luo Y, et al. A novel therapeutic approach for inflammatory bowel disease by exosomes derived from human umbilical cord mesenchymal stem cells to repair intestinal barrier via TSG-6. Stem Cell Res Ther. 2021;12(1):315.

53. Tian J, Kou X, Wang R, Jing H, Chen C, Tang J, et al. Autophagy controls mesenchymal stem cell therapy in psychological stress colitis mice. Autophagy. 2021;17(9):2586–603.

54. Huang Q, Cheng X, Luo C, Yang S, Li S, Wang B, et al. Placental chorionic plate-derived mesenchymal stem cells ameliorate severe acute pancreatitis by regulating macrophage polarization via secreting TSG-6. Stem Cell Res Ther. 2021;12(1):337.

55. Gu G, Lv X, Liu G, Zeng R, Li S, Chen L, et al. Tnfaip6 secreted by bone marrow-derived mesenchymal stem cells attenuates TNBS-induced colitis by modulating follicular helper T cells and follicular regulatory T cells balance in mice. Front Pharmacol. 2021;12: 734040.

56. Wan YM, Li ZQ, Zhou Q, Liu C, Wang MJ, Wu HX, et al. Mesenchymal stem cells alleviate liver injury induced by chronic-binge ethanol feeding in mice via release of TSG6 and suppression of STAT3 activation. Stem Cell Res Ther. 2020;11(1):24.

57. Li Q, Song WJ, Ryu MO, Nam A, An JH, Ahn JO, et al. TSG-6 secreted by human adipose tissue-derived mesenchymal stem cells ameliorates severe acute pancreatitis via ER stress downregulation in mice. Stem Cell Res Ther. 2018;9(1):255.

58. Shin TH, Kim HS, Kang TW, Lee BC, Lee HY, Kim YJ, et al. Human umbilical cord blood-stem cells direct macrophage polarization and block inflammasome activation to alleviate rheumatoid arthritis. Cell Death Dis. 2016;7(12): e2524.

59. Wang S, Lee JS, Hyun J, Kim J, Kim SU, Cha HJ, et al. Tumor necrosis factor-inducible gene 6 promotes liver regeneration in mice with acute liver injury. Stem Cell Res Ther. 2015;6:20.

60. Kota DJ, Wiggins LL, Yoon N, Lee RH. TSG-6 produced by hMSCs delays the onset of autoimmune diabetes by suppressing Th1 development and enhancing tolerogenicity. Diabetes. 2013;62(6):2048–58.

61. Choi H, Lee RH, Bazhanov N, Oh JY, Prockop DJ. Anti-inflammatory protein TSG-6 secreted by activated MSCs attenuates zymosan-induced mouse peritonitis by decreasing TLR2/NF-kappaB signaling in resident macrophages. Blood. 2011;118(2):330–8.

62. Lee RH, Pulin AA, Seo MJ, Kota DJ, Ylostalo J, Larson BL, et al. Intravenous hMSCs improve myocardial infarction in mice because cells embolized in lung are activated to secrete the anti-inflammatory protein TSG-6. Cell Stem Cell. 2009;5(1):54–63.

63. Wisniewski HG, Vilcek J. Cytokine-induced gene expression at the crossroads of innate immunity, inflammation and fertility: TSG-6 and PTX3/TSG-14. Cytokine Growth Factor Rev. 2004;15(2–3):129–46.

64. Day AJ, Milner CM. TSG-6: A multifunctional protein with anti-inflammatory and tissue-protective properties. Matrix Biol. 2019;78–79:60–83.

65. Wisniewski HG, Maier R, Lotz M, Lee S, Klampfer L, Lee TH, et al. TSG-6: a TNF-, IL-1-, and LPS-inducible secreted glycoprotein associated with arthritis. J Immunol. 1993;151(11):6593–601.

Li *et al. Stem Cell Research & Therapy*   (2022) 13:479

Page 15 of 15

66. Lee RH, Yu JM, Foskett AM, Peltier G, Reneau JC, Bazhanov N, et al. TSG-6 as a biomarker to predict efficacy of human mesenchymal stem/progenitor cells (hMSCs) in modulating sterile inflammation in vivo. Proc Natl Acad Sci USA. 2014;111(47):16766–71.
67. Getting SJ, Mahoney DJ, Cao T, Rugg MS, Fries E, Milner CM, et al. The link module from human TSG-6 inhibits neutrophil migration in a hyaluronan- and inter-alpha -inhibitor-independent manner. J Biol Chem. 2002;277(52):51068–76.
68. Song HB, Park SY, Ko JH, Park JW, Yoon CH, Kim DH, et al. Mesenchymal stromal cells inhibit inflammatory lymphangiogenesis in the cornea by suppressing inflammatory macrophage in a TSG-6-dependent manner. Mol Ther. 2018;26(1):162–72.
69. Dyer DP, Thomson JM, Hermant A, Jowitt TA, Handel TM, Proudfoot AE, et al. TSG-6 inhibits neutrophil migration via direct interaction with the chemokine CXCL8. J Immunol. 2014;192(5):2177–85.
70. Dominici M, Le Blanc K, Mueller I, Slaper-Cortenbach I, Marini F, Krause D, et al. Minimal criteria for defining multipotent mesenchymal stromal cells. The International Society for Cellular Therapy position statement. Cytotherapy. 2006;8(4):315–7.
71. Li B, Dewey CN. RSEM: accurate transcript quantification from RNA-Seq data with or without a reference genome. BMC Bioinf. 2011;12:323.
72. Risso D, Schwartz K, Sherlock G, Dudoit S. GC-content normalization for RNA-Seq data. BMC Bioinf. 2011;12:480.
73. Hutchins AP, Yang Z, Li Y, He F, Fu X, Wang X, et al. Models of global gene expression define major domains of cell type and tissue identity. Nucleic Acids Res. 2017;45(5):2354–67.
74. Xu JY, Lee YK, Ran X, Liao SY, Yang J, Au KW, et al. Generation of induced cardiospheres via reprogramming of skin fibroblasts for myocardial regeneration. Stem Cells. 2016;34(11):2693–706.
75. Mittal M, Tiruppathi C, Nepal S, Zhao YY, Grzych D, Soni D, et al. TNFalpha-stimulated gene-6 (TSG6) activates macrophage phenotype transition to prevent inflammatory lung injury. Proc Natl Acad Sci USA. 2016;113(50):E8151–8.
76. Romano B, Elangovan S, Erreni M, Sala E, Petti L, Kunderfranco P, et al. TNF-stimulated gene-6 is a key regulator in switching stemness and biological properties of mesenchymal stem cells. Stem Cells. 2019;37(7):973–87.
77. Kim DK, Choi H, Nishida H, Oh JY, Gregory C, Lee RH, et al. Scalable production of a multifunctional protein (TSG-6) that aggregates with itself and the CHO Cells that synthesize it. PLoS ONE. 2016;11(1): e0147553.
78. Bardos T, Kamath RV, Mikecz K, Glant TT. Anti-inflammatory and chondroprotective effect of TSG-6 (tumor necrosis factor-alpha-stimulated gene-6) in murine models of experimental arthritis. Am J Pathol. 2001;159(5):1711–21.
79. Mindrescu C, Thorbecke GJ, Klein MJ, Vilcek J, Wisniewski HG. Amelioration of collagen-induced arthritis in DBA/1J mice by recombinant TSG-6, a tumor necrosis factor/interleukin-1-inducible protein. Arthritis Rheum. 2000;43(12):2668–77.
80. Watanabe J, Shetty AK, Hattiangady B, Kim DK, Foraker JE, Nishida H, et al. Administration of TSG-6 improves memory after traumatic brain injury in mice. Neurobiol Dis. 2013;59:86–99.

Publisher's Note